

$\lg K_w = -15.56$ for $K_w = [\text{OH}^-][\text{H}_3\text{O}^+]$. The equipment has already been described previously (K. Hegetschweiler, T. Kradolfer, V. Gramlich, R. D. Hancock, *Chem. Eur. J.* **1995**, *1*, 74–88). The computer programs SUPERQUAD (P. Gans, A. Sabatini, A. Vacca, *J. Chem. Soc. Dalton Trans.* **1985**, 1195) and BEST (R. J. Motekaitis, A. E. Martell, *Can. J. Chem.* **1982**, *60*, 2403) were used for evaluation. The complex formation generally took place at such low pH values that hydrolysis of the aqua ions could be neglected.

- [12] Spectrophotometric methods were less suited for the evaluation of these subsequent reactions since the spectra of the various protonated complexes differed only slightly. An evaluation with the program SPECFIT^[14] in the range $3.4 < \text{pH} < 6.4$ yielded the following overall formation constants: $\lg \beta = 23.5(2)$ ($[\text{FeL}]$), $38.2(2)$ ($[\text{FeL}_2]^{3-}$), $44.2(2)$ ($[\text{FeL}(\text{HL})]^{2-}$). The formation of $[\text{Fe}(\text{HL})_2]^-$, which according to potentiometric measurements (Figure 1) is present to an extent of approximately 10% at pH 5, could not be verified with this method.

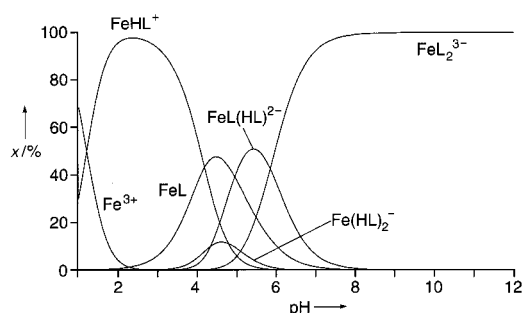


Figure 1. Species distribution (component x [%]) for a complex solution ($[\text{Fe}]_i = 5 \times 10^{-4} \text{ mol dm}^{-3}$, $[\text{L}]_i = 10^{-3} \text{ mol dm}^{-3}$ in $\text{H}_2\text{O}/\text{DMSO}$ (8/2)). Only the Fe-containing species are shown. The formation constants and the $\text{p}K_a$ values from Table 1 were used for the calculations.

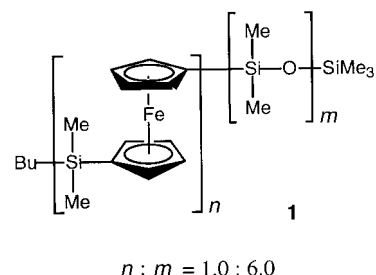
- [13] A species of the composition $\text{Fe}:\text{L}:\text{H} = 1:1:0$ can also be interpreted in terms of a binuclear complex $[(\text{HL})\text{Fe}(\mu\text{-OH})_2\text{Fe}(\text{HL})]$ or $[(\text{HL})\text{Fe}(\mu\text{-O})\text{Fe}(\text{HL})]$ (D. M. Kurtz, Jr., *Chem. Rev.* **1990**, *90*, 585–606). The evaluation of the titration curve according to this model, however, led to less satisfactory agreement ($\sigma_{\text{pH}} = [\sum w(\text{pH}_{\text{found}} - \text{pH}_{\text{calcd}})^2 / \sum w]^{1/2} = 0.0067$ for $[(\text{HL})_2\text{Fe}_2(\text{OH})_2]$, $\sigma_{\text{pH}} = 0.0023$ for $[\text{FeL}]$).
- [14] The determination was performed with solutions of $0.01 < [\text{H}^+] < 0.1 \text{ mol dm}^{-3}$, $[\text{Fe}]_i = [\text{L}]_i = 1.6 \times 10^{-4} \text{ mol dm}^{-3}$, and $\mu = 0.1$ (KNO_3) using a diode array spectrophotometer TIDAS-UVNIR/100-1 from J&M with a HELMA immersion probe and least squares calculations for evaluation (R. A. Binstead, A. D. Zuberbühler, SPECFIT version 2.10, Spectrum Software Associates, Chapel Hill, NC 27515-4494 (USA); see also H. Gampp, M. Maeder, C. J. Meyer, A. D. Zuberbühler, *Talanta* **1985**, *32*, 257–264).
- [15] The measurements were performed at 25°C on a DX17MV instrument (Applied Photophysics).
- [16] The average residence time of a water ligand in $[\text{Al}(\text{OH}_2)_6]^{3+}$ is approximately 150 times higher than for $[\text{Fe}(\text{OH}_2)_6]^{3+}$ (D. T. Richens, *The Chemistry of Aqua Ions*, Wiley, Chichester, **1997**).
- [17] By analogy with the compounds reported by Ryabukhin,^[4] these are probably polymeric complexes. The C,H,N analysis of the Cu complex is in agreement with the formulation $\text{Cu}(\text{HL}) \cdot 2\text{H}_2\text{O}$. To prevent the formation of such solid phases, a competition method was used in which the metal cation M^{2+} was applied in the presence of H_3L as either the nitrilotriacetato (NTA) or iminodiacetato (IDA) complex and converted into the 1:2 complex $[\text{ML}_2]^{4-}$ by addition of KOH. All the necessary $\text{p}K_a$ values and stability constants of H_3NTA and H_2IDA for the $\text{H}_2\text{O}/\text{DMSO}$ system were determined separately.
- [18] R. D. Hancock, *J. Chem. Educ.* **1992**, *69*, 615–621.
- [19] M. Ghisletta, L. Hausherr-Primo, K. Gajda-Schranz, G. Machula, L. Nagy, H. W. Schmalle, G. Rihs, F. Endres, K. Hegetschweiler, *Inorg. Chem.* **1998**, *37*, 997–1008.

Supramolecular Organometallic Polymer Chemistry: Self-Assembly of a Novel Poly(ferrocene)-*b*-polysiloxane-*b*-poly-(ferrocene) Triblock Copolymer in Solution**

Rui Resendes, Jason A. Massey, Hendrik Dorn, K. Nicole Power, Mitchell A. Winnik,* and Ian Manners*

The immiscible segments of a diblock copolymer are known to facilitate self-assembly into a variety of morphologies in the solid state.^[1, 2] In solution, the formation of spherical micelles in a block-selective solvent with a core of the insoluble block surrounded by a corona of the soluble block is well known. However, until recently other morphologies have been rare, and even now the number of systems leading to nonspherical morphologies is limited, and our understanding of them remains poor.^[3, 4] These phenomena provide an attractive and potentially powerful route to nanostructured materials, as illustrated by recent studies of block copolymer films and solution micelles containing metal or semiconductor nanoparticles in desired domains.^[5]

As part of our research on novel poly(ferrocene) block copolymers,^[6, 7] we recently reported studies of the self-assembly of the organometallic–inorganic block copolymer poly(ferrocenyldimethylsilane)-*b*-poly(dimethylsiloxane) (PFS-*b*-PDMS, **1**; PFS:PDMS block ratio 1:6, $M_n = 3.51 \times 10^4$, polymer dispersity index (PDI) = 1.10) in the solid state and in solution.^[8] Thin films of this material self-assemble to form a



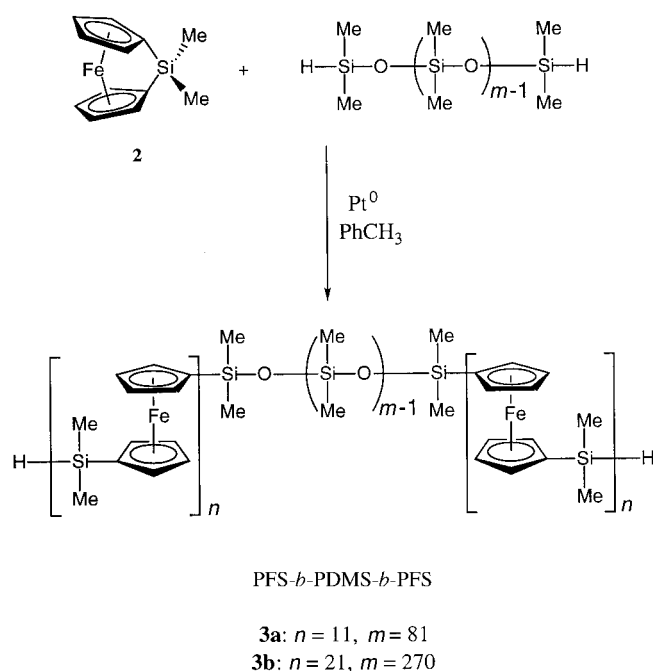
hexagonal array of PFS cylinders within a PDMS matrix, whereas in *n*-hexane, a solvent selective for the PDMS block, cylindrical micelles are formed with a core of PFS surrounded by a sheath of PDMS. As the poly(ferrocene) homopolymer becomes semiconducting on oxidative doping and forms

[*] Prof. M. A. Winnik, Prof. I. Manners, R. Resendes, J. A. Massey, Dr. H. Dorn, K. N. Power
Department of Chemistry
University of Toronto
80 St. George Street
Toronto, Ontario, M5S 3H6 (Canada)
Fax: (+1) 416-978-6157
E-mail: imanners@alchemy.chem.utoronto.ca

[**] This research was supported by the Natural Science and Engineering Research Council of Canada (NSERC). R.R. is grateful for an Ontario Graduate Scholarship, H.D. is grateful to the DFG for a Postdoctoral Fellowship, and K.N.P. is grateful to NSERC for a Postgraduate Scholarship. In addition, I.M. is grateful to the Alfred P. Sloan Foundation for a Research Fellowship (1994–1998), the NSERC for a Stacie Fellowship (1997–1999), and the University of Toronto for a McLean Fellowship (1997–2003).

magnetic ceramics on pyrolysis, these structures represent intriguing prospective precursors to semiconducting or magnetic nanowires.^[9, 10] Here we report the first studies of the self-assembly of a novel organometallic poly(ferrocene) triblock copolymer, PFS-*b*-PDMS-*b*-PFS (**3**, see Scheme 1), which yields multiple and novel morphologies in solution.

The previously studied PFS-*b*-PDMS block copolymer **1** was prepared by sequential living anionic ring-opening polymerization (ROP) of the silicon-bridged [1]ferrocenophane **2** and [Me₂SiO]₃. In contrast, the triblock polymer used in this study (**3**) was prepared by a novel, recently reported transition metal catalyzed ROP approach in which the poly(ferrocene) blocks are “grown” from each end of a poly(dimethylsiloxane) with terminal SiH groups (Scheme 1). This very convenient methodology simply requires the



Scheme 1. Synthesis of PFS-*b*-PDMS-*b*-PFS triblock copolymers **3a** and **3b**.

addition of the [1]ferrocenophane monomer **2** to the commercially available polysiloxane in the presence of a Pt⁰ catalyst (Karstedt's catalyst).^[11] Although the molecular weight distribution obtained by this metal-catalyzed route is broader (PDI typically >1.3 compared to <1.3 by living anionic ROP), we were particularly encouraged by recent studies of an amphiphilic polysilane–poly(ethylene oxide) alternating multiblock copolymer ($M_n = 2.7 \times 10^4$) which demonstrated that despite a fairly broad molecular weight distribution (PDI = 1.6) well-defined supramolecular vesicular aggregates were formed in water.^[12]

The low molecular weight PFS-*b*-PDMS-*b*-PFS block copolymer **3a** was initially prepared as a model to confirm the triblock structure. The polymer was isolated as an orange powder ($M_n = 8.14 \times 10^3$, PDI = 1.45) and characterized by ¹H and ²⁹Si NMR spectroscopy. The data were consistent with the assigned structure. In particular, the absence of a ²⁹Si NMR resonance at $\delta = -6.50$ attributable to the OSiMe₂H end

group of the telechelic PDMS confirmed the proposed triblock structure, and switching groups—groups close to the point where the different blocks meet that show different NMR chemical shifts than analogous groups in the interior of the blocks—between the PFS and PDMS blocks were also apparent. Integration of the ¹H NMR signals indicated that **3a** possessed a PFS:PDMS:PFS block ratio of approximately 1:7:1. A higher molecular weight triblock copolymer (**3b**) with a long PDMS block was then prepared as an amber gum ($M_n = 2.88 \times 10^4$, PDI = 1.43). For this material, integration of the ¹H NMR signals indicated an approximate PFS:PDMS:PFS block ratio of 1:13:1, and differential scanning calorimetry (DSC) analysis revealed thermal transitions close to those of the constituent homopolymers, consistent with phase separation in the solid state ($T_g = 26^\circ\text{C}$: PFS blocks (c.f. 33°C for PFS homopolymer), $T_g = -123^\circ\text{C}$, $T_{\text{cryst}} = -103^\circ\text{C}$, $T_m = -44^\circ\text{C}$: PDMS blocks).

The solution aggregation of **3b** was studied in *n*-hexane, a good solvent for PDMS and a precipitant for PFS. Preliminary dynamic light scattering studies on a solution of **3b**, prepared by heating the material in *n*-hexane at 80°C for 1 h, suggested the presence of large aggregates (diameter ca. 60 nm on average) in solution. A micellar solution was then prepared by first dissolving **3b** in THF, a good solvent for both blocks, and subsequently adding *n*-hexane very slowly until micelles formed. The resulting solution was then dialyzed against pure *n*-hexane to remove the THF. Transmission electron microscopy (TEM) studies of this micellar solution, after solvent evaporation, revealed three main, coexistent morphologies. Specifically, **3b** was found to assemble into spherical micelles, cylindrical micelles, and also novel flowerlike structures^[13] (Figure 1). As TEM relies on contrast provided by electron density differences, this technique allowed the selective imaging of the iron-containing PFS cores. Analysis of the dialyzed solution in *n*-hexane by atomic force microscopy (AFM) allowed both the PFS cores and the PDMS coronas to be visualized, and showed the presence of spherical micelles (Figure 2a) and large globular assemblies (Figure 2b) consist-

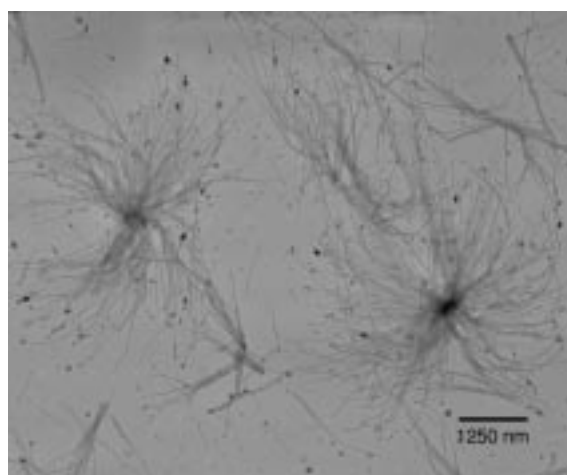


Figure 1. Transmission electron micrograph obtained by aerosol spraying a dilute, dialyzed solution of **3b** in hexane onto a thin carbon film supported on mica. It was not necessary to stain the sample as the iron-rich domains provided sufficient contrast. The micrograph revealed three distinct and coexistent micellar morphologies.

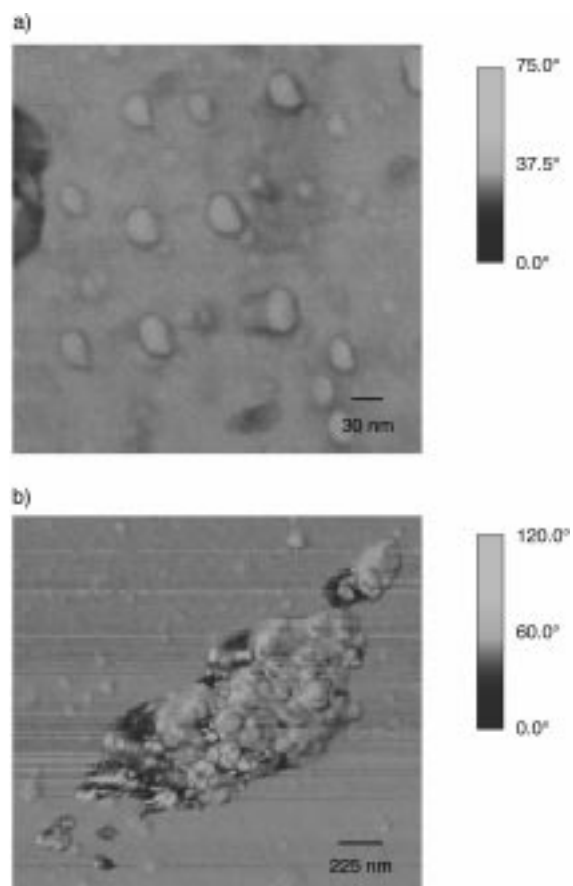


Figure 2. AFM micrographs (phase image) of a) spherical micelles and b) flowerlike micelles of **3b** (dialyzed solution in *n*-hexane).

tent in size and shape with the flowerlike micellar cores observed by TEM.

To investigate the influence of the composition variation present in samples of **3b** on the observed morphology, fractionation was performed.^[14] Centrifugation (1.5×10^4 rpm for 20 min) of the dialyzed solution of **3b** in *n*-hexane resulted in the formation of a two-phase system with a very light, amber supernatant and a yellow precipitate. Analysis of the supernatant by TEM after solvent evaporation showed it to be composed almost entirely of spherical micelles (Figure 3a). ¹H NMR integration of this sample gave an approximate PFS:PDMS:PFS block ratio of 1:60:1, indicative of a much smaller PFS content compared to the unfractionated sample. Analysis by gas-phase chromatography (GPC) revealed this fraction to be of lower molecular weight ($M_n = 2.52 \times 10^4$, PDI = 1.50; Figure 4). In contrast, TEM analysis of a solution of the above-mentioned yellow precipitate in *n*-hexane, after solvent evaporation, showed it to be made up predominantly of flowerlike and short cylindrical micelles (Figure 3b). Integration of the ¹H NMR signals for this sample revealed a PFS:PDMS:PFS block ratio of approximately 1:6:1, consistent with a significantly higher PFS content compared to the unfractionated sample. Analysis of this fraction by GPC revealed a higher molecular weight ($M_n = 3.97 \times 10^4$, PDI = 1.37; Figure 4). These initial observations suggest that, in contrast to the polysilane–polyethylene oxide system mentioned above, the variation in the relative

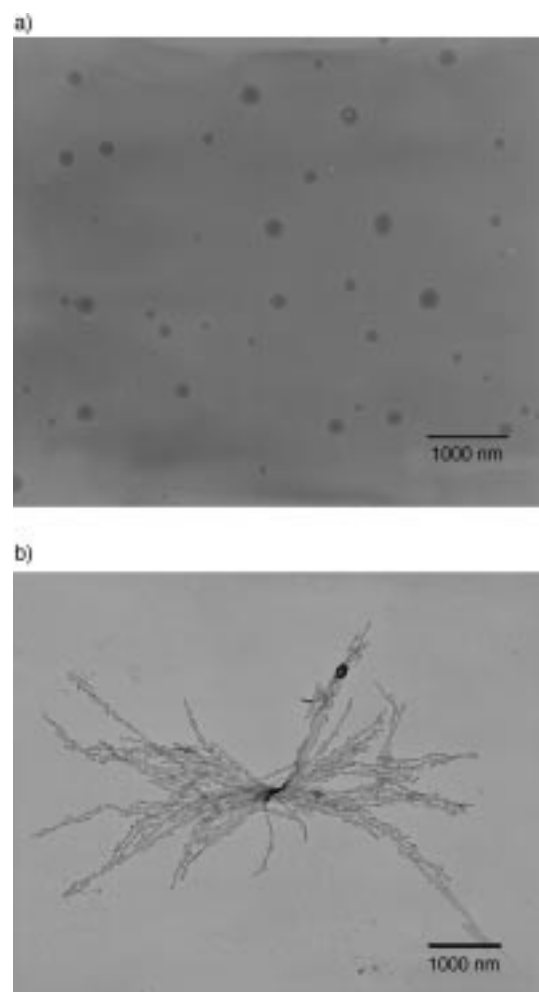


Figure 3. Transmission electron micrographs of a) supernatant and b) re-dissolved precipitate obtained from the centrifugation experiment. Samples were prepared by aerosol spraying a dilute solution in hexane onto a thin carbon film supported on mica. It was not necessary to stain the samples as the iron-rich domains provided sufficient contrast.

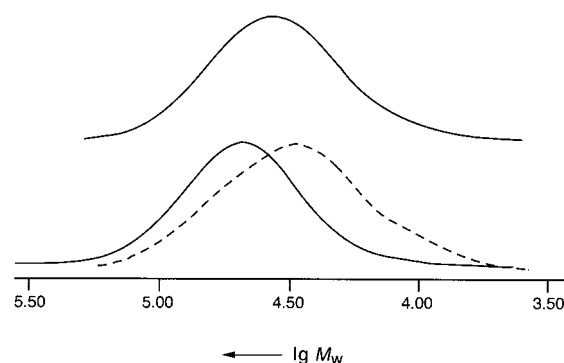


Figure 4. GPC traces of bulk **3b** (upper solid line) as well as the high molecular weight fraction (lower solid line) and low molecular weight fraction (dashed line) derived from the centrifugation experiment.

block lengths present in the sample is critical in determining the observed micellar morphologies in this organometallic–inorganic triblock system.

In summary, the first studies of the self-assembly of a poly(ferrocene) triblock copolymer, which was obtained by a facile transition metal catalyzed ROP, have illustrated the reproducible^[14] formation of multiple morphologies and, in

particular, the formation of novel flowerlike structures. The observation of coexisting multiple morphologies in diblock copolymer systems of narrow polydispersity has been previously reported,^[15] whereas (as mentioned above) recent work has provided examples of systems in which well-defined aggregates are formed despite significant polydispersities ($PDI = 1.6$).^[12] In our particular case, fractionation experiments suggest that the composition variations associated with the polydispersity of the sample ($PDI = 1.4$) play a critical role in determining the morphologies observed. Future work will focus on gaining further detailed understanding of the factors that influence the formation of the observed supramolecular organometallic polymer structures. In addition, PFS is redox-active: Upon oxidation it becomes a semiconductor, and on pyrolysis it forms magnetic ceramics. Therefore, the possibility of accessing nanoscale assemblies with intriguing physical properties is also of considerable interest.^[9,10]

Experimental Section

Samples for TEM were prepared by aerosol spraying a dilute micellar solution (ca. 50 μL , ca. 10^{-4} mg mL^{-1}) onto a thin carbon film (ca. 10 \AA) grown on mica and then floated off the mica and placed on 200-mesh gilder copper TEM grids. Transmission electron micrographs were obtained on a Hitachi model 600 electron microscope. Samples for AFM were prepared by aerosol spraying a dilute micellar solution (ca. 50 μL , ca. 10^{-4} mg mL^{-1}) onto freshly cleaved mica. The AFM images were obtained using a Nanoscope III microscope (Digital Instruments) in the tapping mode with a silicon cantilever with a resonance frequency of 300–380 kHz. The GPC data were obtained in THF and are relative to polystyrene standards, and the values are therefore considered to be estimates.

3a: To a solution of **2** (1.16 g, 4.79 mmol) and SiH-terminated PDMS (1.44 g, 0.24 mmol, $M_w = 6.02 \times 10^3$, $PDI = 1.24$) in toluene (20 mL) was added an aliquot (43 μL) of a 0.3% (by weight) solution of Karstedt's catalyst in xylenes. After stirring for 24 h, the deep orange solution was precipitated into methanol (150 mL). The orange precipitate was washed with methanol (3×100 mL) and dried under vacuum. Yield: 1.95 g (75%). GPC: $M_n = 8.14 \times 10^3$, $PDI = 1.45$; $^1\text{H NMR}$ (400 MHz, C_6D_6): $\delta = 0.28$ (s, 21H, $\text{OSi}(\text{CH}_3)_2\text{O}$), 0.54 (s, 6H, $\text{fcSi}(\text{CH}_3)_2\text{fc}$), 4.09 (m, 4H, α - or β - C_5H_4), 4.26 (m, 4H, α - or β - C_5H_4); $^{29}\text{Si}\{^1\text{H}\}$ NMR (79.5 MHz, C_6D_6 , DEPT $J = 51$ Hz): $\delta = -21.4$ (s, $\text{OSi}(\text{CH}_3)_2\text{O}$), -18.2 (s, $\text{fcSi}(\text{CH}_3)_2\text{H}$), -6.38 (s, $\text{fcSi}(\text{CH}_3)_2\text{fc}$), 0.7 (s, $\text{fcSi}(\text{CH}_3)_2\text{O}$); $\text{fc} = (\text{C}_5\text{H}_4)_2\text{Fe}$.

3b: To a solution of **2** (1.73 g, 7.14 mmol) and SiH-terminated PDMS (5.0 g, 0.25 mmol, $M_w = 2.00 \times 10^4$, $PDI = 1.60$ (GPC)) in toluene (40 mL) was added an aliquot (64 μL) of a 0.3% (by weight) solution of Karstedt's catalyst in xylenes. After stirring for 24 h, the deep orange solution was precipitated into methanol (250 mL). The adhesive orange gum was washed with methanol (3×200 mL) and dried under vacuum. Yield: 4.8 g (71%). GPC: $M_n = 2.88 \times 10^4$, $PDI = 1.43$; $^1\text{H NMR}$ (400 MHz, C_6D_6): $\delta = 0.28$ (s, 39H, $\text{OSi}(\text{CH}_3)_2\text{O}$), 0.55 (s, 6H, $\text{fcSi}(\text{CH}_3)_2\text{fc}$), 4.10 (m, 4H, α - or β - C_5H_4), 4.27 (m, 4H, α - or β - C_5H_4); $^{29}\text{Si}\{^1\text{H}\}$ NMR (79.5 MHz, C_6D_6 , DEPT $J = 51$ Hz): $\delta = -21.4$ (s, $\text{OSi}(\text{CH}_3)_2\text{O}$), -6.4 (s, $\text{fcSi}(\text{CH}_3)_2\text{fc}$).

Received: March 15, 1999 [Z13163IE]

German version: *Angew. Chem.* **1999**, *111*, 2738–2742

Keywords: copolymerizations • nanostructures • polymers • self-assembly • supramolecular chemistry

[1] S. Förster, M. Antonietti, *Adv. Mater.* **1998**, *10*, 495.

[2] F. S. Bates, *Science* **1991**, *251*, 898.

[3] J. P. Spatz, S. Mössmer, M. Möller, *Angew. Chem.* **1996**, *108*, 1673; *Angew. Chem. Int. Ed. Engl.* **1996**, *35*, 1510.

- [4] For recent work on nonspherical micellar aggregates of organic block copolymers in solution, see for example C. Price, *Pure Appl. Chem.* **1983**, *55*, 1563; M. Antonietti, S. Heinz, M. Schmidt, C. Rosenauer, *Macromolecules* **1994**, *27*, 3276; L. Zhang, A. Eisenberg, *Science* **1995**, *268*, 1728; L. Zhang, K. Yu, A. Eisenberg, *Science* **1996**, *272*, 1777; Y. Yu, A. Eisenberg, *J. Am. Chem. Soc.* **1997**, *119*, 8383; J. Tao, S. Stewart, G. Liu, M. Yang, *Macromolecules* **1997**, *30*, 2738.
- [5] For recent intriguing examples of nanostructured materials based on block copolymers, see S. Förster, M. Antonietti, *Adv. Mater.* **1998**, *10*, 195; C. C. Cummins, R. R. Schrock, R. E. Cohen, *Chem. Mater.* **1992**, *4*, 27; G. Liu, J. Ding, *Adv. Mater.* **1998**, *10*, 69; G. Liu, *Adv. Mater.* **1997**, *9*, 437; K. L. Wooley, *Chem. Eur. J.* **1997**, *3*, 1397; M. Moffitt, H. Vali, A. Eisenberg, *Chem. Mater.* **1998**, *10*, 1021; J. Spatz, S. Mössmer, M. Möller, M. Kocher, D. Neher, G. Wegner, *Adv. Mater.* **1998**, *10*, 473.
- [6] R. Rulkens, Y. Ni, I. Manners, *J. Am. Chem. Soc.* **1994**, *116*, 12 121.
- [7] Y. Ni, R. Rulkens, I. Manners, *J. Am. Chem. Soc.* **1996**, *118*, 4102.
- [8] J. Massey, K. N. Power, I. Manners, M. A. Winnik, *J. Am. Chem. Soc.* **1998**, *120*, 9533.
- [9] a) I. Manners, *Can. J. Chem.* **1998**, *76*, 371; b) J. Massey, K. N. Power, M. A. Winnik, I. Manners, *Adv. Mater.* **1998**, *12*, 1559; c) I. Manners, *Chem. Commun.* **1999**, 857.
- [10] In addition, the formation of magnetic nanostructures upon pyrolysis of cylinders of PFS in mesoporous silica, MCM-41, has been demonstrated; see for example M. J. MacLachlan, P. Aroca, N. Coombs, I. Manners, G. A. Ozin, *Adv. Mater.* **1998**, *10*, 144.
- [11] P. Gómez-Elipé, R. Resendes, P. M. Macdonald, I. Manners, *J. Am. Chem. Soc.* **1998**, *120*, 8348.
- [12] S. J. Holder, R. C. Hiorns, N. A. J. M. Sommerdijk, S. J. Williams, R. G. Jones, R. J. M. Nolte, *Chem. Commun.* **1998**, 1445.
- [13] Similar morphologies have been observed in the precipitation of calcium phosphate in the presence of double-hydrophilic block copolymers: M. Antonietti, M. Breulmann, C. G. Göltner, H. Cölfen, K. K. W. Wong, D. Walsh, S. Mann, *Chem. Eur. J.* **1998**, *4*, 2493.
- [14] To investigate the reproducibility of micelle formation as well as the possible separation of the different micellar morphologies, an additional micellar solution was prepared employing the same dialysis methodology mentioned above. When this solution of **3b** in *n*-hexane was examined by TEM after solvent evaporation the same micellar assemblies were observed.
- [15] K. Yu, A. Eisenberg, *Macromolecules* **1996**, *29*, 6359.

Identification of Triplet States in Carotenoids by Intracavity Absorption Spectroscopy and Measurements of Delayed Fluorescence**

Hans Bettermann,* Lars Ulrich, Gabriele Domnick, and Hans-Dieter Martin

Carotenoids have two important functions in nature: the absorption of solar energy and the subsequent radiationless energy transfer to chlorophyll or bacteriochlorophyll at the beginning of photosynthesis as well as the quenching of triplet states of chlorophyll, which generate singlet oxygen, and the quenching of already generated singlet oxygen. While it has

[*] Priv.-Doz. Dr. H. Bettermann, Dipl.-Chem. L. Ulrich
Institut für Physikalische Chemie und Elektrochemie der Universität
Universitätsstrasse 1, D-40225 Düsseldorf (Germany)
Fax: (+49) 211-8115195
E-mail: betterma@uni-duesseldorf.de
Dipl.-Chem. G. Domnick, Prof. Dr. H.-D. Martin
Institut für Organische Chemie und Makromolekulare Chemie der
Universität Düsseldorf (Germany)

[**] We are grateful to the Fonds der Chemischen Industrie for financial support.